

In-Context Positive-Unlabeled Learning

Siyan Liu, Yi Chang, Manli Cheng, Qinglong Tian, and Pengfei Li

Department of Statistics and Actuarial Science, University of Waterloo

Abstract

Positive-unlabeled (PU) learning addresses binary classification when only a set of labeled positives is available alongside a pool of unlabeled samples drawn from a mixture of positives and negatives. Existing PU methods typically require dataset-specific training or iterative optimization, which limits their applicability when many tasks must be solved quickly or with little tuning. We introduce **PUICL**, a pretrained transformer that solves PU classification entirely through in-context learning. PUICL is pretrained on synthetic PU datasets generated from randomly instantiated structural causal models, exposing it to a wide range of feature-label relationships and class-prior configurations. At inference time, PUICL receives the labeled positives and the unlabeled samples as a single input and returns class probabilities for the unlabeled rows in one forward pass, with no gradient updates or per-task fitting. On 20 semi-synthetic PU benchmarks derived from the UCI Machine Learning Repository, OpenML, and scikit-learn, PUICL outperforms four standard PU learning baselines in average AUC and accuracy, and is competitive on F_1 -score. These results show that the in-context learning paradigm extends naturally beyond fully supervised tabular prediction to the semi-supervised PU setting.

1 Introduction

1.1 Positive and Unlabeled Data

Positive and unlabeled (PU) data arise when only a subset of positive examples is labeled, while the remaining data consist of a mixture of positive and negative instances. Such settings are common in many applications, including medical research, ecology, and machine learning. For example, in contaminated case-control studies, diagnosed patients form a labeled positive group, while the control group, which is intended to contain healthy individuals, may include undiagnosed cases, resulting in contamination. Similarly, in ecological studies, presence-only data record observed occurrences of a species, while unobserved locations remain unlabeled rather than truly negative. Analogous structures also appear in applications such as text classification, recommendation systems, and medical screening, where positive labels can be obtained with high confidence but reliable negative labels are difficult or costly to acquire.

A standard assumption in PU learning is the *selected completely at random* (SCAR) assumption, which posits that the conditional feature distribution of the positive class is identical for labeled and unlabeled positives. Under SCAR, the observed data follow

$$\begin{aligned}\mathbf{x}_1, \dots, \mathbf{x}_n &\sim f_+(\mathbf{x}), \\ \mathbf{x}_{n+1}, \dots, \mathbf{x}_{n+m} &\sim (1 - \pi) f_+(\mathbf{x}) + \pi f_-(\mathbf{x}),\end{aligned}$$

where $\pi \in (0, 1)$ denotes the negative prevalence in the unlabeled pool, and $f_+(\mathbf{x})$ and $f_-(\mathbf{x})$ are the feature distributions of the positive and negative classes, respectively. In practice, all three quantities are unknown.

The goal of PU learning is to construct a classifier that distinguishes positive from negative instances using only PU data. This problem is inherently more challenging than standard supervised classification due to the absence of fully observed negative samples. As a result, successful methods must exploit the mixture structure of the unlabeled data together with the information provided by labeled positives, making PU learning a distinctive form of semi-supervised learning.

1.2 In-context Learning

Modern large language models (LLMs), such as ChatGPT, do not retrain their parameters for each new task. Instead, they adapt their predictions based on examples or instructions provided in the input, all within a single forward pass. This phenomenon is known as *in-context learning* (ICL). More broadly, ICL refers to a paradigm in which a pretrained model adapts to a new prediction task using the data supplied at inference time, without any parameter updates.

From a statistical perspective, ICL suggests an alternative mode of learning. Rather than fitting a new model separately for each dataset, as in conventional supervised learning, one can instead train a general-purpose prediction mechanism that learns to condition on data and perform inference directly. This paradigm has recently shown strong empirical success across a variety of domains.

1.3 Related Work

PU Learning Most existing work on PU learning has focused on prediction, particularly on training classifiers from data containing only positive and unlabeled examples. Early work by [Elkan and Noto \[2008\]](#) introduced a probabilistic formulation of PU classification, which led to a large body of classifier-oriented approaches. These include risk-reweighting and unbiased risk estimation methods [[du Plessis et al., 2014](#), [Kiryo et al., 2017](#)], approaches that incorporate additional structural assumptions such as known class priors [[Hido et al., 2011](#), [Kato et al., 2019](#)], and methods based on the anchor set assumption and its variants [[Chen et al., 2020](#), [Garg et al., 2021](#)]. Despite their differences, these methods all operate within the standard (semi-)supervised learning paradigm, where a model is explicitly trained or optimized for each dataset.

Tabular Foundation Models Recent work on tabular foundation models has shifted the paradigm of tabular learning from dataset-specific training to in-context learning. In this framework, a pretrained model receives the training data as context and produces predictions for new observations in a single forward pass. A representative example is TabPFN [[Hollmann et al., 2025](#)], which pretrains a transformer on synthetic prior data and demonstrates strong performance on small tabular classification tasks without per-dataset optimization.

Beyond TabPFN, several recent models have expanded this paradigm toward improved scalability and realism. For instance, TabICL [[Qu et al., 2025](#)] introduces a two-stage architecture that enables efficient in-context learning on substantially larger datasets, while TabDPT [[Ma et al., 2025](#)] emphasizes pretraining on real tabular data and exhibits favorable scaling behavior with respect to both model and data size. These developments suggest that tabular foundation models are evolving into a general-purpose framework for tabular prediction.

1.4 Our Contributions

We introduce **PUICL**, a pretrained transformer model for PU learning that operates entirely through in-context learning. Unlike existing PU methods, which require dataset-specific model fitting or iterative optimization, PUICL performs classification in a single forward pass without updating model parameters. This represents a fundamental shift in how PU learning problems can be approached, replacing per-dataset training with a general-purpose inference mechanism learned through pretraining.

From the perspective of tabular foundation models, our work extends their applicability beyond standard supervised learning to the semi-supervised setting. While existing models such as TabPFN focus primarily on supervised prediction, PUICL demonstrates that the in-context learning paradigm can be successfully adapted to problems with incomplete labeling, thereby broadening the scope of tabular foundation models.

On the methodological side, we develop a prior data generation procedure specifically tailored to PU learning, enabling effective pretraining under the in-context framework. The model adopts a TabPFN-style transformer architecture and is trained using a curriculum designed to improve robustness across diverse data regimes. To facilitate reproducibility and future research, we make the entire pipeline fully open-source, including the prior data generation process, training curriculum, and model implementation.

The rest of this paper is organized as follows. Section 2 describes the prior data generation procedure based on randomly instantiated structural causal models, together with the construction of synthetic PU training instances. Section 3 presents the PUICL architecture and explains how the input encoding, dual-axis transformer, and output decoder are adapted to the PU setting. Section 4 details the pretraining curriculum and the in-context inference procedure. Section 5 reports empirical results on 20 semi-synthetic PU classification tasks and compares PUICL against four standard PU learning baselines. Section 6 concludes with a discussion of limitations and future directions.

2 Prior Data Generation

To pretrain the model in-context, we require a distribution over labeled datasets that captures the diversity of real-world PU learning problems. We construct this prior using randomly instantiated structural causal models (SCMs), following the meta-learning prior philosophy of [Hollmann et al. \[2025\]](#), [Qu et al. \[2025\]](#). Each training step draws a fresh synthetic dataset from this prior, exposing the model to a wide variety of data-generating mechanisms without any real labeled data.

2.1 SCM Construction.

Each dataset is generated by a distinct SCM, instantiated as a randomly initialized multilayer perceptron (MLP). Concretely, the SCM consists of k exogenous (root) variables, a depth- L_g MLP with hidden dimension h , and two readout heads for features and labels respectively. The MLP weights are drawn independently from $\mathcal{N}(0, \sigma_{\text{init}}^2)$ with zero biases, and the activation function of each hidden layer is drawn uniformly from a fixed bank of ten nonlinearities: tanh, ReLU, GELU, the identity $\phi(x) = x$, the sign function $\phi(x) = \text{sign}(x) \in \{-1, 0, 1\}$, the Heaviside step function $\phi(x) = \mathbf{1}[x > 0]$, a radial basis function $\phi(x) = \exp(-x^2)$, the sine function $\phi(x) = \sin(x)$, the square function $\phi(x) = x^2$, and the absolute value $\phi(x) = |x|$. Because a new MLP is instantiated for every dataset, the collection of all such MLPs implicitly defines a rich nonparametric prior over functional relationships between inputs and outputs.

2.2 Forward Pass, Feature and Label Generation

To generate n samples, we first draw exogenous cause vectors $\mathbf{u}_i \in \mathbb{R}^k$ i.i.d. from $\mathcal{N}(\mathbf{0}, \mathbf{I})$ (or $\text{Uniform}(0, 1)^k$, depending on the configuration). These are propagated through the MLP as follows. Let $\mathbf{h}_i^{(0)} = \mathbf{W}_0 \mathbf{u}_i$ be the output of the input linear layer. For each subsequent layer $\ell = 1, \dots, L_g - 1$:

$$\mathbf{h}_i^{(\ell)} = \mathbf{W}_\ell \phi_\ell(\mathbf{h}_i^{(\ell-1)}) + \boldsymbol{\varepsilon}_i^{(\ell)}, \quad \boldsymbol{\varepsilon}_i^{(\ell)} \sim \mathcal{N}(\mathbf{0}, \sigma_{\text{noise}}^2 \mathbf{I}),$$

where ϕ_ℓ is the activation function of layer ℓ . The per-layer Gaussian noise $\boldsymbol{\varepsilon}_i^{(\ell)}$ introduces stochasticity into the functional relationships, reflecting the fact that real SCMs are rarely deterministic.

How the feature vector $\mathbf{x}_i \in \mathbb{R}^d$ and the latent label score $s_i \in \mathbb{R}$ are jointly extracted depends on the chosen generation mode. In the *non-causal* mode, both quantities are read off from the final hidden state $\mathbf{h}_i^{(L_g-1)}$ via dedicated linear readout heads: a feature readout $\mathbf{R}_x \in \mathbb{R}^{d \times h}$ yields $\mathbf{x}_i = \mathbf{R}_x \mathbf{h}_i^{(L_g-1)}$, and a label readout $\mathbf{r}_y \in \mathbb{R}^h$ yields $s_i = \mathbf{r}_y^\top \mathbf{h}_i^{(L_g-1)}$. Alternatively, the features can be set directly to the exogenous causes, $\mathbf{x}_i = \mathbf{u}_i$ (requiring $d = k$), while the label score is still produced by the label readout; this bypasses the MLP nonlinearities for the features entirely. In the *causal* mode, no readout heads are used. Instead, all intermediate hidden states $\mathbf{h}_i^{(1)}, \dots, \mathbf{h}_i^{(L_g-1)}$ are concatenated into a single pool of $(L_g - 1)h$ latent variables, each corresponding to an endogenous node in the SCM. One node is selected uniformly at random to serve as the label variable s_i , restricted to either the first hidden block (placing the label at a causally upstream position) or the last hidden block (placing it at a causally downstream position). The d feature variables \mathbf{x}_i are then selected from the remaining nodes, either as a contiguous clique surrounding the label node (to preserve dense local causal dependencies) or as a random subset drawn without replacement from the full pool. This construction ensures that features and label are genuine intermediate nodes of the SCM, with their relationships governed entirely by the network’s weight matrices and activation functions.

In all modes, each feature dimension and the score are independently standardized to zero mean and unit variance across the n samples and clipped to $[-20, 20]$ for numerical stability. Binary labels are then assigned by ranking samples on s_i : the top $\lceil \pi n \rceil$ samples are designated as *negatives* ($y_i = -$), while the remaining samples are designated as *positives* ($y_i = +$), where $\pi \in (0, 1)$ is the target negative prevalence. This rank-based thresholding ensures that the label is a deterministic, monotone function of the latent score, with classification difficulty governed entirely by the geometry of the SCM.

2.3 Constructing the PU Training Set

The fully labeled dataset is converted into a PU learning instance by the following strategy. We generate one binary-labeled dataset of size $n = n_{\text{tr}} + n_u$ and split it into two portions: a *pre-removal training portion* of size n_{tr} and an *unlabeled portion* of size n_u , both containing positive ($y = +$) and negative ($y = -$) samples. We then remove all negatives from the training portion, leaving only P positives, which serve as the labeled positive data. The unlabeled portion has its labels hidden and is presented to the model as unlabeled data. Combining these two components yields a PU dataset that mimics realistic PU learning scenarios, where only a small set of confirmed positives is available alongside a large pool of unlabeled data of unknown composition.

This process is governed by three parameters: the number of labeled positives P , the unlabeled-to-positive ratio $\eta > 0$, and the negative prevalence $\pi \in (0, 1)$ shared by both the training portion and the unlabeled set. Since the pre-removal training portion contains P positives at a positive prevalence of $1 - \pi$, its size is $n_{\text{tr}} = \lceil P / (1 - \pi) \rceil$, of which $\pi \cdot n_{\text{tr}}$ negatives are removed after the

split. The unlabeled set size is $n_u = \lceil P \cdot \eta \rceil$. To form the split with controlled class composition, the positive and negative samples are partitioned into separate pools, shuffled independently, and allocated to each portion such that the realized negative prevalence in both portions approximates π . The final PU dataset presented to the model consists of P labeled positives and n_u unlabeled samples whose labels are hidden during training and revealed only for evaluation.

3 Model Architecture

We adopt a tabular transformer architecture modified from [Hollmann et al. \[2025\]](#), [Pfefferle et al. \[2025\]](#) for the PU learning setting. The model takes a PU dataset as input, which consists of P labeled positives and n_u unlabeled samples, each with d features, and outputs a class probability for each unlabeled sample, all in a single forward pass without any gradient update at inference time. Figure 1 illustrates the flow of a PU dataset through the model architecture.

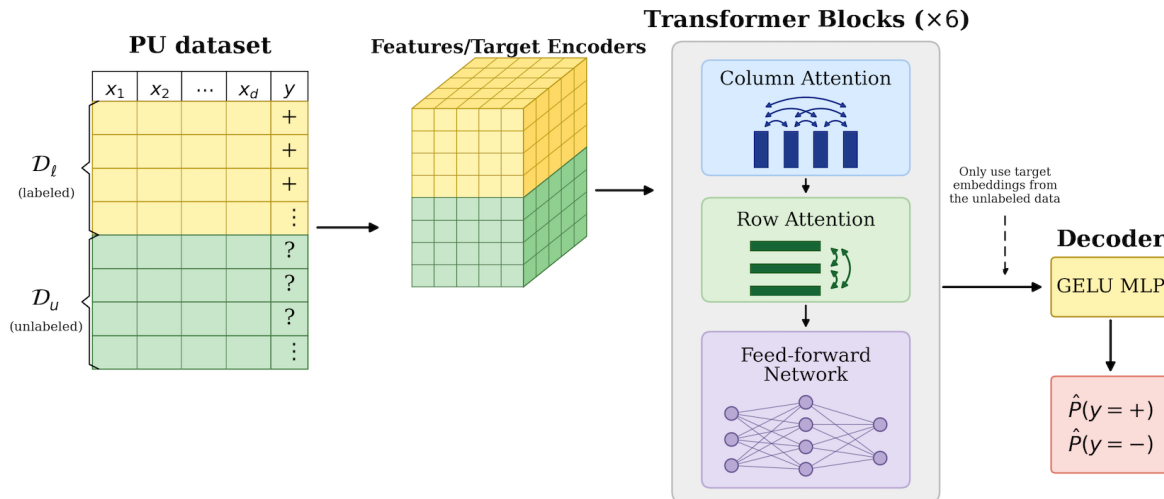


Figure 1: Architecture of the in-context PU learning model. The input PU dataset $\mathcal{D}_\ell \cup \mathcal{D}_u$, where \mathcal{D}_ℓ denotes the set of P labeled positives and \mathcal{D}_u the set of n_u unlabeled samples, is encoded into a 4-D embedding tensor of shape $B \times n \times (d+1) \times e$ (batch size, rows, columns, embedding dimension), processed by L transformer blocks each applying column attention (across features), row attention (across data points), and a feed-forward layer, and finally decoded into class probabilities $\hat{P}(y=+)$ and $\hat{P}(y=-)$ for each unlabeled sample via a GELU MLP applied to the unlabeled-row target embeddings.

3.1 Input Encoding

The input dataset is represented as a matrix of $n_u + P$ rows and $d + 1$ columns, where the extra column holds the label. Each entry of this matrix is a scalar, and the model embeds every scalar independently into a vector of dimension e (the embedding size) before any attention is applied.

Feature encoder. Each feature value x_{ij} (the value of feature j for sample i) is encoded by a single shared linear layer $\mathbf{W}_x \in \mathbb{R}^{1 \times e}$. Before projection, each feature column is standardized using

the mean and standard deviation computed from the labeled positive rows only, and clipped to $[-100, 100]$.

Target encoder. The label column requires special treatment because unlabeled samples have no observed label. For labeled positives, the label scalar is projected by a linear layer $\mathbf{w}_y \in \mathbb{R}^{1 \times e}$, identical in form to the feature encoder. For unlabeled samples, a dedicated encoding is needed.

Models like TabPFN [Hollmann et al., 2025] handle unobserved test labels by imputing them with the mean of the training labels. In standard supervised in-context learning this is benign. In the PU setting, however, all labeled training examples are positives, so the mean label is a constant. Imputing every unlabeled entry with this constant would assign them all the same positive-class encoding, making the model unable to distinguish positives from negatives among the unlabeled samples, which will result in a fundamental identifiability failure.

We therefore replace mean imputation with a learnable *unlabeled token* $\mathbf{v} \in \mathbb{R}^e$, a globally shared parameter trained jointly with the rest of the model. This token is used as the label embedding for every unlabeled sample, regardless of its true (hidden) class. Rather than injecting a fixed, potentially misleading signal, the unlabeled token allows the model to learn, through pretraining, the most informative representation for an entry whose label is unknown in a PU context.

Input fusion. The d feature embeddings and the single label embedding for each row are concatenated along the column dimension, yielding a 4-D representation $\mathbf{H}^{(0)} \in \mathbb{R}^{B \times n \times (d+1) \times e}$, where B is the batch size and $n = P + n_u$ is the total number of rows. This representation can be thought of as a table of embedding vectors, with one vector per cell.

3.2 Dual-Axis Transformer

The core of the model is a stack of L transformer encoder blocks, each of which applies two successive multi-head self-attention operations along orthogonal axes of the table, followed by a position-wise feed-forward network.

Within-row attention (between features). The first attention operation is applied independently to each row. The table is reshaped to $(B \cdot n) \times (d + 1) \times e$, so that each row becomes a sequence of $d + 1$ token embeddings (one per feature plus the label). Multi-head self-attention is applied across these tokens, allowing the model to capture interactions among features and between features and the label within a single sample. The output is reshaped back to the full table and passed through a layer normalization.

Within-column attention (between data points). The second attention operation is applied independently to each column. The table is transposed and reshaped to $(B \cdot (d + 1)) \times n \times e$, so that each column becomes a sequence of n row embeddings. Multi-head self-attention is then applied across all n rows without any masking, enabling every sample, either labeled or unlabeled, to attend to every other sample in the dataset.

This design departs from the attention masking scheme used in models like TabPFN [Hollmann et al., 2025]. In standard supervised in-context learners, test samples are treated as *external* queries: training-set representations are computed independently of the test inputs, and test samples are prevented from attending to one another, since each test prediction should be conditionally independent given the training context. Such masking reflects the assumption that the test set plays no role in defining the learned function.

PU learning, however, is fundamentally a semi-supervised problem. The unlabeled samples are not external queries but an integral part of the learning problem: the global structure of the unlabeled pool carries information that is directly relevant to identifying positives within it. Predictions are therefore *within-dataset* rather than out-of-sample, and unlabeled samples should be allowed to inform one another. We accordingly remove all attention masks and allow unrestricted full self-attention across all rows, so that labeled and unlabeled samples jointly shape each other’s representations throughout every layer of the network.

Feed-forward sublayer. Each block concludes with a standard position-wise feed-forward network applied to every cell embedding:

$$\mathbf{H} \leftarrow \mathbf{W}_2 \text{GELU}(\mathbf{W}_1 \mathbf{H}) + \mathbf{H},$$

where $\mathbf{W}_1 \in \mathbb{R}^{e \times e_{\text{ff}}}$ and $\mathbf{W}_2 \in \mathbb{R}^{e_{\text{ff}} \times e}$, followed by layer normalization.

3.3 Output Decoder

After L transformer blocks, predictions are read from the label-column embeddings of the unlabeled rows only. Formally, for each unlabeled row i , the model extracts the embedding at the label-column position, $\mathbf{z}_i^{(L)} \in \mathbb{R}^e$, and passes it through a two-layer MLP decoder:

$$\hat{\mathbf{p}}_i = \mathbf{W}_4 \text{GELU}(\mathbf{W}_3 \mathbf{z}_i^{(L)}),$$

where $\hat{\mathbf{p}}_i \in \mathbb{R}^2$ are the logits for the positive ($y=+$) and negative ($y=-$) classes. The model is trained with a cross-entropy loss computed over the unlabeled rows, whose true labels are available from the synthetic prior but withheld from the model during the forward pass.

3.4 Model Configuration

The default model configuration uses an embedding size of $e = 128$, $L = 6$ transformer blocks, 8 attention heads, and a feed-forward hidden size of $e_{\text{ff}} = 256$. The model has no positional encoding, consistent with the permutation-invariant nature of tabular data: predictions should not depend on the order in which samples or features are presented. Under this configuration, the model has approximately 1.23 million trainable parameters in total, which is several orders of magnitude smaller than typical large language models, and comparable in scale to a small convolutional network. The bulk of these parameters (1.19M, or 97%) reside in the six transformer blocks; the feature and target encoders together contribute fewer than 650 parameters, and the output decoder contributes 33,538. This extreme compactness is a direct consequence of the in-context learning paradigm: rather than encoding task-specific knowledge in a large number of weights, the model is trained to read and reason over the dataset presented at inference time, delegating the burden of adaptation entirely to the attention mechanism. The result is a lightweight predictor that generalizes across PU learning problems without any per-task fine-tuning.

4 Pretraining and Inference

4.1 Pretraining

The model is trained entirely on synthetic PU datasets sampled from the SCM prior described in Section 2; no real labeled data are used at any point during training. Each training step draws a

fresh batch of 24 independent datasets per GPU (effective batch size 48 across two GPUs), computes predictions for the unlabeled rows, and minimizes the cross-entropy loss against the withheld true labels. Training proceeds in two phases totaling $K_{\text{tot}} = 100,000$ gradient steps, completed in approximately 15 hours on a single node with two NVIDIA H100 GPUs using data-parallel distributed training.

Phase 1: data curriculum. The first phase runs for $K = 100$ stages of 750 steps each (75,000 steps total). Within each stage, the SCM architecture is fixed to a randomly drawn configuration: the number of hidden layers is sampled uniformly from $\{4, \dots, 12\}$ and the hidden width from $\{12, \dots, 36\}$. A separate set of factors is resampled independently for every batch, including noise level $\sigma_{\text{noise}} \in \{0.005, 0.01, 0.02\}$, input distribution (Gaussian or uniform), activation schedule, feature-source mode, and feature ordering, providing broad coverage of the prior support regardless of stage. The number of input features per dataset is drawn uniformly from $\{5, \dots, 20\}$ and the number of labeled positives from $\{100, \dots, 300\}$, both sampled fresh every step.

The stage index controls the difficulty of the PU composition. Two quantities are annealed linearly from stage 1 to stage $K = 100$:

- **Unlabeled-to-positive ratio** $\eta = n_u/P$: begins fixed at $\eta = 1$ and by the final stage is drawn uniformly from $[0.5, 2.0]$, exposing the model to datasets with varying balance between the labeled and unlabeled pools.
- **Negative prevalence** π : begins fixed at 0.5 and by the final stage is drawn uniformly from $[0.1, 0.9]$, training the model to handle the full spectrum from nearly pure-positive to nearly pure-negative unlabeled sets.

In addition, the probability that the generating SCM is causal increases linearly with the stage index s as $P(\text{causal}) = s/(2K)$, reaching 0.5 at the last stage. Early training is therefore dominated by the simpler non-causal regime, with causal datasets introduced gradually.

Phase 2: final-stage tail. After the curriculum, training continues for an additional 25,000 steps with all PU-composition parameters fixed at their final-stage ranges ($\eta \sim \mathcal{U}[0.5, 2.0]$, $\pi \sim \mathcal{U}[0.1, 0.9]$). The learning rate is scaled down by a factor of 4 relative to Phase 1 (peak 4×10^{-5} , floor 4×10^{-6} , with a 2,000-step linear warmup). This tail phase allows the model to consolidate representations under the hardest distribution without further curriculum drift.

Optimizer and learning rate schedule. Both phases use the AdamW optimizer with $\beta_1=0.9$, $\beta_2=0.95$, and weight decay 10^{-4} . Gradients are clipped to unit ℓ_2 norm. In Phase 1, the learning rate follows a linear warmup over the first 4,000 steps to a peak of 1.6×10^{-4} , then decays polynomially with exponent 1.5 to a floor of 1.6×10^{-5} . An exponential moving average of the model weights with decay 0.95 is maintained throughout both phases and used for all evaluation and inference.

4.2 Inference

At test time the model receives a PU dataset consisting of P labeled positives and n_u unlabeled samples, and produces a probability estimate $\hat{P}(y=+ | \mathbf{x})$ for each unlabeled sample in a single forward pass. No gradient computation, fine-tuning, or dataset-specific optimization is performed; the model generalizes purely through the in-context mechanism learned during pretraining.

5 Experiments

In this section, we investigate the performance of the proposed PUICL method ¹ on PU classification. For comprehensive evaluations, we first describe several baseline methods and then discuss the empirical results.

5.1 Settings

Baseline methods. We compare our proposed PUICL with four baseline methods: **EMPU** [Liu et al., 2025], **VPU** [Chen et al., 2020], unconstrained least-squares importance fitting (**uLSIF**) [Hido et al., 2011], and **(TED)ⁿ** [Garg et al., 2021].

- **EMPU** [Liu et al., 2025] is a semiparametric PU learning method that formulates PU learning through density-ratio modeling and estimates the model parameters using an expectation-maximization (EM) algorithm, providing a closely related baseline for density-ratio-based PU learning.
- **VPU** [Chen et al., 2020] is a class-prior-free variational PU learning method that characterizes the gap between a given classifier and the Bayes classifier.
- **uLSIF** [Hido et al., 2011] is a kernel-based density-ratio estimation method that directly estimates the importance weights between two distributions. Since uLSIF is not specifically designed for PU learning, we adapt it as a density-ratio baseline for PU classification.
- **(TED)ⁿ** [Garg et al., 2021] is an iterative transform-estimate-discard framework for PU learning. This method combines best-bin estimation of the negative prevalence π with the conditional value ignoring risk (CVIR) objective and serves as a recent mixture-based PU learning baseline.

Data synthesis and models. A total of 20 semi-synthetic PU classification tasks are constructed from real-world binary tabular datasets, including benchmark datasets from the UCI Machine Learning Repository, OpenML, and scikit-learn. After preprocessing each dataset, the majority class is treated as the positive class. To control the task size, at most 600 positive observations are sampled and then split into labeled and unlabeled positives in a 1:2 ratio, so that approximately one third of the positives are labeled and the remaining two thirds are unlabeled. Negative observations are then added to the unlabeled pool to target a negative prevalence of $\pi = 0.5$; equivalently, when sufficient negatives are available, the number of unlabeled negatives is matched to the number of unlabeled positives. Thus, when the positive cap is reached, each PU task contains approximately 200 labeled positives, 400 unlabeled positives, and 400 unlabeled negatives, while smaller datasets are adjusted according to the available numbers of positive and negative observations.

Evaluation metrics. To evaluate the performance, for each synthetic dataset, we evaluate all methods using three standard metrics: area under the receiver operating characteristic curve (AUC), classification accuracy (Acc), and F_1 -score. AUC assesses ranking performance without requiring a fixed classification cutoff, whereas Acc and F_1 -score evaluate the resulting class-label predictions. To reduce the effect of random sampling variability, the data generation and evaluation procedure is repeated 10 times.

¹An implementation of PUICL is publicly available at <https://anonymous.4open.science/r/puicl-58B1>.

Ranking metric: AUC. A score function $r(\mathbf{x}) := \hat{P}(y = + | \mathbf{x})$ can be obtained from PUICL and all four baselines, and is used to compute the empirical AUC via the Mann–Whitney U statistic:

$$\widehat{\text{AUC}} = \frac{1}{n_u^{(-)} n_u^{(+)}} \sum_{i: y_{u,i}=+} \sum_{j: y_{u,j}=-} [I\{r(\mathbf{x}_i) > r(\mathbf{x}_j)\} + \frac{1}{2} I\{r(\mathbf{x}_i) = r(\mathbf{x}_j)\}],$$

where $n_u^{(+)}$ and $n_u^{(-)}$ are the numbers of positive and negative units in the unlabeled set, respectively, and $y_{u,i}$ is the true label of the i -th unlabeled observation (revealed only at evaluation).

Classification metrics: Acc and F_1 -score. We further evaluate classification performance using Acc and the F_1 -score. Acc is defined as the proportion of correctly classified observations in the test set. The F_1 -score, defined as the harmonic mean of precision and recall, summarizes the trade-off between these two quantities, where precision is the proportion of predicted positives that are truly positive, and recall is the proportion of true positives that are correctly identified. For PU data, the F_1 -score emphasizes the ability to recover the positive class, whereas Acc measures overall classification accuracy.

5.2 Results and Analysis

The empirical results on the 20 semi-synthetic PU classification tasks are summarized in Table 1. The table reports the AUC, accuracy (Acc), and F_1 -score for all competing methods, with the highest value for each dataset and each metric highlighted in bold.

In terms of AUC, PUICL consistently demonstrates strong performance among the five competing methods. It achieves the highest AUC on the majority of datasets and also attains the largest cross-dataset average AUC (0.882), as shown in the last row. Among the baseline methods, uLSIF is the most competitive in average AUC, with an average value of 0.841, followed by (TED)ⁿ and EMPU with average AUC values of 0.832 and 0.824, respectively. VPU obtains a lower average AUC of 0.752, although it performs strongly on some individual datasets such as MONK-1.

For classification performance, Acc and F_1 -score are reported for the four methods that provide explicit class predictions. PUICL achieves the best average Acc (0.802) and attains the highest Acc on most datasets. For the F_1 -score, PUICL remains highly competitive, with an average value of 0.758, which is close to the best average value of 0.759 achieved by (TED)ⁿ. Notably, PUICL achieves the highest F_1 -score on the majority of datasets, indicating strong performance in identifying the positive class. Overall, these results demonstrate that PUICL delivers robust and well-balanced performance across different evaluation metrics, combining strong ranking ability with competitive classification accuracy in PU learning.

6 Discussion

We introduced PUICL, a transformer-based model that solves PU classification entirely through in-context learning. Pretrained on synthetic datasets generated from randomly instantiated structural causal models, PUICL takes a labeled-positive set and an unlabeled pool as a single input and returns class probabilities in one forward pass, with no gradient updates or per-task fitting. PUICL outperforms four standard PU learning baselines in average AUC and accuracy and is competitive on F_1 -score, while remaining compact at roughly only 1.23M trainable parameters.

Several limitations should be acknowledged. First, the prior generation procedure encodes the SCAR assumption, so PUICL inherits the misspecification that affects most SCAR-based PU methods when the labeling mechanism is informative. Second, the model is trained with at most 20

Table 1: Average AUC, accuracy (Acc), and F_1 -score of competing methods on 20 semi-synthetic PU classification tasks. The best result for each dataset and metric is highlighted in **bold**. PUICL consistently achieves strong performance across datasets, particularly in terms of AUC and accuracy.

| Dataset | AUC | | | | | Acc | | | | F_1 -score | | | |
|----------------|--------------|--------------|--------------|-------|--------------------|--------------|--------------|--------------|--------------------|--------------|--------------|--------------|--------------------|
| | PUICL | EMPU | VPU | uLSIF | (TED) ⁿ | PUICL | EMPU | VPU | (TED) ⁿ | PUICL | EMPU | VPU | (TED) ⁿ |
| Diabetes | 0.809 | 0.789 | 0.782 | 0.786 | 0.759 | 0.714 | 0.666 | 0.670 | 0.690 | 0.690 | 0.677 | 0.586 | 0.694 |
| Haberman | 0.685 | 0.674 | 0.612 | 0.666 | 0.649 | 0.682 | 0.527 | 0.673 | 0.645 | 0.395 | 0.452 | 0.290 | 0.473 |
| Heart | 0.871 | 0.842 | 0.732 | 0.862 | 0.846 | 0.759 | 0.722 | 0.655 | 0.774 | 0.784 | 0.757 | 0.609 | 0.779 |
| ILPD | 0.723 | 0.696 | 0.667 | 0.619 | 0.610 | 0.645 | 0.576 | 0.618 | 0.596 | 0.419 | 0.586 | 0.038 | 0.461 |
| MONK-1 | 0.846 | 0.743 | 0.895 | 0.813 | 0.796 | 0.727 | 0.726 | 0.772 | 0.720 | 0.729 | 0.663 | 0.790 | 0.723 |
| MONK-2 | 0.824 | 0.506 | 0.600 | 0.638 | 0.625 | 0.671 | 0.539 | 0.558 | 0.595 | 0.489 | 0.269 | 0.482 | 0.559 |
| MONK-3 | 0.975 | 0.846 | 0.936 | 0.942 | 0.955 | 0.780 | 0.718 | 0.782 | 0.901 | 0.823 | 0.750 | 0.818 | 0.904 |
| Abalone | 0.900 | 0.900 | 0.876 | 0.879 | 0.882 | 0.810 | 0.811 | 0.790 | 0.801 | 0.802 | 0.810 | 0.773 | 0.796 |
| Adult | 0.855 | 0.820 | 0.500 | 0.826 | 0.796 | 0.762 | 0.721 | 0.500 | 0.733 | 0.756 | 0.732 | 0.000 | 0.732 |
| Banknote | 1.000 | 0.999 | 1.000 | 1.000 | 1.000 | 0.989 | 0.980 | 0.980 | 0.993 | 0.989 | 0.980 | 0.981 | 0.993 |
| Car | 0.919 | 0.735 | 0.796 | 0.784 | 0.794 | 0.846 | 0.702 | 0.763 | 0.791 | 0.642 | 0.403 | 0.482 | 0.579 |
| Default Credit | 0.724 | 0.663 | 0.500 | 0.703 | 0.657 | 0.652 | 0.610 | 0.500 | 0.629 | 0.616 | 0.579 | 0.000 | 0.620 |
| Iranian Churn | 0.952 | 0.904 | 0.667 | 0.909 | 0.899 | 0.857 | 0.778 | 0.577 | 0.832 | 0.867 | 0.812 | 0.290 | 0.831 |
| Letter C vs U | 0.999 | 0.992 | 0.993 | 0.991 | 0.996 | 0.977 | 0.925 | 0.942 | 0.974 | 0.978 | 0.930 | 0.945 | 0.974 |
| MAGIC Gamma | 0.897 | 0.799 | 0.795 | 0.870 | 0.847 | 0.808 | 0.710 | 0.701 | 0.773 | 0.808 | 0.671 | 0.698 | 0.771 |
| Mushroom | 0.993 | 0.959 | 0.952 | 0.968 | 0.962 | 0.966 | 0.873 | 0.857 | 0.940 | 0.967 | 0.887 | 0.864 | 0.940 |
| Rice | 0.975 | 0.978 | 0.500 | 0.970 | 0.966 | 0.913 | 0.921 | 0.500 | 0.911 | 0.910 | 0.922 | 0.000 | 0.910 |
| Spambase | 0.913 | 0.888 | 0.745 | 0.856 | 0.889 | 0.819 | 0.786 | 0.671 | 0.806 | 0.835 | 0.811 | 0.649 | 0.826 |
| WDBC | 0.994 | 0.976 | 0.900 | 0.978 | 0.987 | 0.955 | 0.775 | 0.839 | 0.950 | 0.953 | 0.820 | 0.783 | 0.947 |
| Wine Quality | 0.780 | 0.764 | 0.586 | 0.758 | 0.729 | 0.702 | 0.657 | 0.531 | 0.674 | 0.710 | 0.648 | 0.254 | 0.673 |
| Average | 0.882 | 0.824 | 0.752 | 0.841 | 0.832 | 0.802 | 0.736 | 0.694 | 0.786 | 0.758 | 0.708 | 0.517 | 0.759 |

features, a few hundred labeled positives, and class priors restricted to $\pi \in [0.1, 0.9]$; performance outside this regime—particularly for high-dimensional data or extreme class imbalance—is not guaranteed. Third, although PUICL implicitly reasons about the mixture composition of the unlabeled pool, it does not return an explicit estimate of π , which limits its use in applications requiring calibrated decision thresholds or interpretable class priors. These limitations suggest several directions for future work. The prior could be extended to incorporate explicit selection mechanisms, enabling PUICL to handle non-SCAR data. Architecture and prior extensions would enable scaling to larger feature dimensions and sample sizes, while augmenting the output head with a class-prior estimator and calibration module would yield interpretable π estimates. Finally, the in-context formulation extends naturally to other forms of weak supervision, suggesting that PUICL is a first step toward a broader family of in-context semi-supervised tabular learners.

References

- Hui Chen, Fangqing Liu, Yin Wang, Liyue Zhao, and Hao Wu. A variational approach for learning from positive and unlabeled data. *Advances in Neural Information Processing Systems*, 33: 14844–14854, 2020.
- Marthinus C. du Plessis, Gang Niu, and Masashi Sugiyama. Analysis of learning from positive and unlabeled data. *Advances in Neural Information Processing Systems*, 27:703–711, 2014.
- Charles Elkan and Keith Noto. Learning classifiers from only positive and unlabeled data. In *Proceedings of the 14th ACM SIGKDD international conference on Knowledge discovery and data mining*, pages 213–220, 2008.

- Saurabh Garg, Yifan Wu, Alexander J Smola, Sivaraman Balakrishnan, and Zachary Lipton. Mixture proportion estimation and PU learning: a modern approach. *Advances in Neural Information Processing Systems*, 34:8532–8544, 2021.
- Shohei Hido, Yuta Tsuboi, Hisashi Kashima, Masashi Sugiyama, and Takafumi Kanamori. Statistical outlier detection using direct density ratio estimation. *Knowledge and Information Systems*, 26(2):309–336, 2011.
- Noah Hollmann, Samuel Müller, Lennart Purucker, Arjun Krishnakumar, Max Körfer, Shi Bin Hoo, Robin Tibor Schirrmeyer, and Frank Hutter. Accurate predictions on small data with a tabular foundation model. *Nature*, 637(8045):319–326, 2025.
- Masahiro Kato, Takeshi Teshima, and Junya Honda. Learning from positive and unlabeled data with a selection bias. In *International Conference on Learning Representations*, 2019.
- Ryuichi Kiryo, Gang Niu, Marthinus C du Plessis, and Masashi Sugiyama. Positive-unlabeled learning with non-negative risk estimator. *Advances in Neural Information Processing Systems*, 30, 2017.
- Siyan Liu, Chi-Kuang Yeh, Xin Zhang, Qinglong Tian, and Pengfei Li. Positive and unlabeled data: model, estimation, inference, and classification. *Journal of the American Statistical Association*, 120(552):2547–2558, 2025.
- Jian Ma, Valentin Thomas, Rasa Hosseinzadeh, Alex Labach, Hamidreza Kamkari, Jesse C. Cresswell, Kouros Golestan, Guangwei Yu, Anthony L. Caterini, and Maksims Volkovs. TabDPT: scaling tabular foundation models on real data. *Advances in Neural Information Processing Systems*, 2025.
- Alexander Pfefferle, Johannes Hog, Lennart Purucker, and Frank Hutter. nanotabpfn: A lightweight and educational reimplement of tabpfn. *arXiv preprint arXiv:2511.03634*, 2025.
- Jun Qu, David Holzmüller, Gaël Varoquaux, and Marine Le Morvan. TabICL: A tabular foundation model for in-context learning on large data. In *Proceedings of the 42nd International Conference on Machine Learning*, volume 267, pages 50817–50847. PMLR, 2025.